INTL JOURNAL OF ELECTRONICS AND TELECOMMUNICATIONS, 2025, VOL. 71, NO. 1, PP. 197–202
Manuscript received August 24, 2024; revised March, 2025. doi: 10.24425/ijet.2025.15354962

Design of Ultra Compact Optical T Flip Flop in Two Dimensional Photonic Crystals

Mahesh V Sonth, Jyoti B, Sanjaykumar C Gowre, Savita Soma, and Juhi Nishat Ansari

***Abstract*—The research in the field of quantum electronics is gaining more momentum over the solid state physics device design. In the proposed research we have designed an ultra compact optical T flip-flop in two dimensional (2-D) photonic crystals (PhCs) on a rectangular lattice with 16×9 dielectric rods in air configuration. The principle mechanism used here is adding an extra input called reference input to achieve logic high for no power applied at the input of T flip-flop. The two junctions are created for guiding the light wave towards the output. The reference input and one refractive index varied dielectric rod placed near the junction to confine the ouput power along with T input. At the junction of the input-output we have used the constructive and destructive interference method to achieve maximum light confinement in the output. The plane wave expansion (PWE) method is used to compute the photonic band gap (PBG) and the finite difference time domain (FDTD) method is used to analyze electromagnetic (EM) wave propagation inside the waveguides. The time for input arrival at the output also significantly improved with reduction in the chip size. The response time for the proposed T flip-flop is 0.0049 ps and contrast ratio achieved is 13.60 dB with a chip area of 49.5 μm^2.**

***Keywords*—T flip-flop, Photonic crystals, FDTD, PWE, Contrast ratio**

I. Introduction

TODAYS fast correspondence world is confronting a ton of limits in view of slow execution of electric gadgets. Optical components will be utilized in future as an answer for this issue. Optical components give huge data transfer capacity, low power utilization and high exchanging speed. In recent past, conventional electronic devices have been replaced by optical devices because of its rich properties such as low power consumption, higher switching operations, and large bandwidth [1]. So nowadays all optical devices are extensively used in photonic integrated circuits, optical networks and optical signal processing [2].

Literature supports many design technologies which has its own challenges, few of those are highlighted here. Semiconductor optical Amplifiers faces an issue of noise effect and speed of operation. Elevated input power is the necessity for phC ring resonators [3]. While interferometers based designs suffers from complex integration. Optical fibers faces an issue of chip scale integration [4], [5].In order to handle these drawbacks all optical devices based on photonic crystal waveguides [6] are used as it offers small size, less power consumption and robust light confinement, so all optical devices are generally implemented by photonic crystal waveguides (PhCWs). Many optical logical gates like NOT, OR, AND, NAND and NOR [7]–[10], devices like filters [11], encoders and decoders [12], [13], mux, demux [14]–[16], adders [17], [18] and flip flops [19]–[23].

In optical routing, optical computing and optical shift registers all-optical flip-flops (AOFFs) are used as a storage element. Various mechanisms are used to implement AOFFs. Mach Zehnder Interferometer (MZI) method is used to realize AOFFs but it have an issue of complex integration. The flip-flop is realized by Polarization switch by using polarization rotation effect of semiconductor optical amplifier (SOA) method, it faces an issue of spontaneous noise [24].Coupled laser diodes method and semiconductor distributed feedback laser (DFBL) [25], [26] is used to implement AOFFs but these devices under go with holding beam. In this research we have designed all optical T FF in 2D PhCs and is compuationally verified its functionality in optical domain using FDTD and PWE method.

II. Methods and Materials

A. Defect Mechanisms in 2-D PhCs for waveguides

There are two kinds of defects: line defects and point defects. A defect is produced by upsetting a solitary lattice site along a line in the z direction. This deformity has broken the evenness of the periodic dielectric constant. It causes a restriction of light or a set of intently oriented modes to a point in the plane of propagation. These models include recurrence inside the band gap. This unsettling influence is known as a point defect or cavity. In simple words, a cavity is encircled by reflecting walls that don't permit getting away from light, which subsequently prompts mode. There are number of ways,

VGST, Bangalore, Karnataka State, India under award no. VGST/K-FIST (L1) (2014-15)/ (2015-16)/373 has supported this work.

Mahesh V Sonth is with School of Electrical and Communication Sciences, JSPM University, Pune-412207, Maharashtra, India (email: mvs.secs@jspmuni.ac.in).

Jyoti B is with Department of ECE, Bheemanna Khandre Institute of Technology, Bhalki-585328, Karnataka, India (e-mail: jyotipatil129@gmail.com).

Sanjaykumar C Gowre is with School of Electrical & Communication Sciences, JSPM University Pune -412207, Maharashtra, India (e-mail: scg.secs@jspmuni.ac.in).

Savita Soma is with Department of ECE, Guru Nanak Dev Engineering College, Bidar-585403, Karnataka, India (e-mail: savita.soma@gmail.com).

Juhi Nishat Ansari is with Department of ECE, K.C.T. Engineering College, Kalaburagi-585104, Karnataka, India (e-mail: juhi.nishat.ansari@gmail.com).

like supplant the single column with another size, shape or dielectric constant than the first or eliminate a column from the crystal as displayed in figure 1(a).

A distinct defect is a linear defect. It is utilized to direct the light starting with one position and then onto the next. The principal thought is to frame a waveguide from the PhC by changing a direct series of crystals, as displayed in figure 1(b). Light with the recurrence in the PBG that spreads in the waveguide is bound to the deformity and can be coordinated along the defect. The construction with the linear defect actually has one direction in which discrete translational balance is preserved inside the plane. The system of directing light is index guiding, that is, total internal reflection in the ordinary dielectric wave guides; however, this system binds the line just in the area of higher -ϵ. For this situation, the system of direction is PBG, which is free of the material's properties that are filled in the center. This property is significant for the quantity of uses wherein a decrease in collaboration between the light and dielectric material is required.

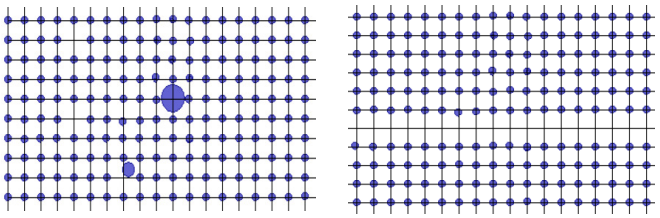

(a) (b)

Fig. 1. Defects in 2D PhCs: (a) distant ways of point defects, (b) linear defect

The distinction between a linear defect and point defect isn't just that were talked about before. A mode is confined just when its recurrence inside PBG for a point defect. A mode isn't just the capability of recurrence; additionally, it is wave vector for the linear defect. There is a need to characterize the mix of wave vector and recurrence for the directed mode. There are a number of ways in which linear defects can be presented in the PhCs. So there are a number of directed modes. The main condition is to keep up with the discrete transnational balance in one course. This can be accomplished by eliminating each nth rod or each rod along a solitary rod. This results in a solitary mode wave guide that has just a single directed mode at the given recurrence. The second way is by eliminating each rod along different rows of rods, which results in a multi-mode wave guide. This is bothersome for the utilization of data transmission since the signal goes with the numerous velocities, which brings about modal scattering. The PhC shows different cross-section designs, such as hexagonal, triangular, cubic, circular, and square. Every one of them having their own evenness focuses. The waveguides in 2-D PhCs play a vital role in the construction of all optical device.

The different types of waveguides that can be created in 2-D PhCs are planar waveguides. These waveguides can be created in different ways, such as: (i) By deleting the entire row in the lattice structure (ii) The row with a smaller rod radius compared to other rows, the structures are shown in figure 2. The Quadratic T waveguide and Cross waveguide,

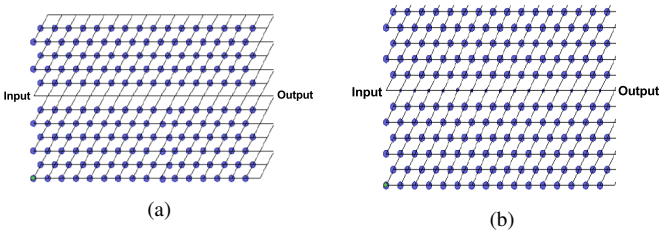

(a) (b)

Fig. 2. Planar waveguides: (a) one complete row is eliminated, (b) one complete row rods are minimised

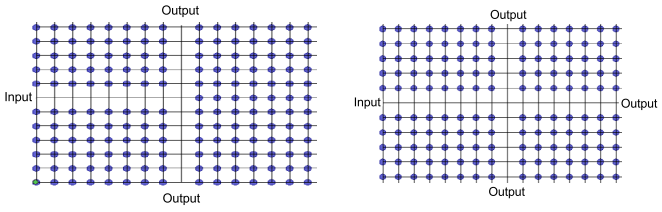

(a) (b)

Fig. 3. Quadratic waveguides: (a) t waveguide, (b) cross waveguide

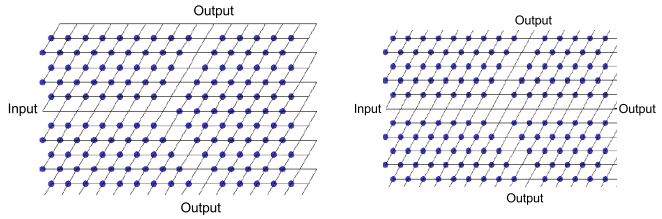

(a) (b)

Fig. 4. Triangular waveguides: (a) two split, (b) three split

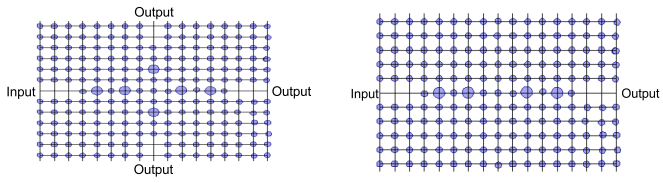

(a) (b)

Fig. 5. Hybrid waveguides: (a) quadratic, (b) planar

Triangular split waveguide and Planar Hybrid waveguide are shown in figures 3, 4, 5.

B. *Mathematical Modeling*

The band gap of a PhC describes the disallowed frequencies of the light through the structure. A complete PBG is a range of frequencies ω in which there are no propagation solutions (real k) of Maxwell's equations for any vector k and it is surrounded by propagation states above and below the forbidden gap. The light photons are a composition of time varying E and H fields. When these photons interact with the PhC structure boundaries, their propagation behavior is governed by Maxwell equations. James Clerk Maxwell brought together various laws of electrostatics and steady magnetic fields.There are 4 Maxwell's equations. They relate

E and H field variables in time varying and static fields.

$$\bigtriangledown \times E = \frac{\partial B}{\partial t} \tag{1}$$

$$\bigtriangledown \times H = \frac{\partial B}{\partial t} + J \tag{2}$$

$$\bigtriangledown \cdot D = \rho_v \tag{3}$$

$$\bigtriangledown \cdot B = 0 \tag{4}$$

To analyze and understand the E and H fields propagation through the 2D PhC structure proposed in this article, the required Maxwell's equations are to be solved with necessary medium and boundary conditions. Let us assume the medium is isotropic, non-magnetic, and charge free. The constitutive equations relate field intensites E and H with flux densites D and B respectively, and whose precise form depends on the material in which the fields exist. They are given by

$$D(x,z,t) = \epsilon_0 \epsilon_r(x,z) E(x,z,t) \tag{5}$$

$$B(x,z,t) = \mu_0 H(x,z,t) \tag{6}$$

Where ϵ_0 and μ_0 are the permittivity and permeability of free space, respectively, ϵ_r (x,z) is the relative permittivity of the dielectric material that varies periodically in the xz plane. In free space μ=μ_0 = $4\pi \times 10^{-7}$ H/m, ϵ_0 = 8.854×10^{-12} F/m. The two curl equations for the waves propagating in a periodic time varying media on the xz plane are

$$\bigtriangledown \times E(x,z,t) = -\partial_t B(x,z,t) \tag{7}$$

$$\bigtriangledown \times H(x,z,t) = \partial_t D(x,z,t) \tag{8}$$

where ∂_u = $\frac{\partial}{\partial u}$. Since it is a 2D PhC in xz plane, no dielectric variation in y-direction i.e., - ∂_t=0 and $\bigtriangledown$= $a_x\ \partial_x$+ $a_z\ \partial_z$. The corresponding harmonic waves in frequency domain with frequency ω are

$$\bigtriangledown \times E(x,z) = -j\omega\mu_0 H(x,z) \tag{9}$$

$$\bigtriangledown \times H(x,z) = j\omega\epsilon_0\epsilon_r(x,z) E(x,z) \tag{10}$$

Dividing Eqn.(10) by $\epsilon_r(x,z)$ and taking curl on both sides, we get

$$\bigtriangledown \times \frac{1}{\epsilon_r(x,z)} \bigtriangledown \times H(x,z) = \bigtriangledown \times j\omega\epsilon_0 E(x,z) \tag{11}$$

Using the Eqn.(9) we can write Eqn.(11) as

$$\bigtriangledown \times \frac{1}{\epsilon_r(x,z)} \bigtriangledown \times H(x,z) = \left(\frac{\omega}{c}\right)^2 H(x,z) \tag{12}$$

where c = $\frac{1}{\sqrt{(\epsilon_0\mu_0)}}$ = 3×10^8 m/s, is the speed of light in vaccum.

Eqn.(12) is called the Master's equation for steady state in dielectric medium [27]. Using this master equation the complete band diagram for the specific PhC structure can be computed. Eqn.12 can be used to compute all the electromagnetic fields in PhC structures. Considering PhC structures with periodic arrangement of dielectric material, we can express the electric field E(r), magnetic field H(r), and dielectric permittivity ϵ(r) in terms of their Fourier series coefficients as

$$E(r) = \sum_G E_G e^{i(k+G).r}, H(r) = \sum_G H_G e^{i(k+G).r},$$
$$\epsilon(r) = \sum_G \epsilon_G e^{i(k+G).r} \tag{13}$$

Here E_G, H_G and ϵ_G are periodic functions with periodicity of lattice. And the indices indicate that the periodic function is different for each wave vector k and number of Eigen-state n. To depict the dispersion graph of the PhC structure, the PWE method isused. In this method, an eigenvalue equation is formed by substituting the Fourier series expansion of the periodic function into Eqn. (12). In the given 2DPhC, the dielectric function ϵ_r (x,z)varies periodically in x and z directions and is uniform in y direction. The inverse of the dielectric constant and Bloch modes are explained in Fourier series upon the reciprocal vector of the lattice, G, which is given as

$$\eta(x,z) = \frac{1}{\epsilon(x,z)} = \sum_G \eta_G e^{(jk.(x,z))} \tag{14}$$

Waves in a periodic medium can propagate with no scattering and their behavior is ruled by a periodic envelop function which is multiplied by a plane wave. The Fourier series expansion of the magnetic field in terms of plane wave basis with the help of Bloch's theorem gives

$$H(x,z) = \sum_G u_G^{n,k} e^{j(k+G).(x,z)} \tag{15}$$

Substituting above two equations in Master equation, we get

$$\sum_G \eta_{G-G'}(K+G') \times [(k+G) \times u_{G'}^{n,k}] = \frac{w_n(k)^2}{c^2} u_{G'}^{n,k} \tag{16}$$

On simplification of Eqn.(16) gives an eigenvalue equation from which we obtain the band diagram of the periodic structure. In the eigenvalue equation, the wave vector k enters as a parameter that has a continuous variation in the first Brillouin Zone. Brillouin zone boundaries represent Bragg planes which reflect (diffract) waves having particular wave vectors. Simply stated Brillouin zone is the region of all allowed wave vectors of k. The plot of wave vector versus mode frequency gives the dispersion diagram.

C. Thoery of T flip flop

The flip-flop is a two stable state circuit, used to store the binary data. These are the basic elementary unit of any digital system. T flip-flop is a altered form of JK flip-flop, It is designed by combining the J and K inputs and created a single input called T. Hence it is also called as single input JK flip-flop.

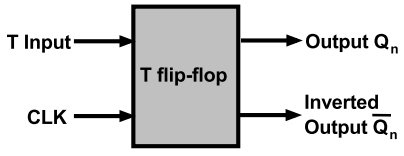

Fig. 6. T flip-flop

T flip- flops are able to find the complement of its state when T=1, so it is also called the Toggle flip-flop and it maintain the same state when T is zero. The T flip- flop to toggle its

output, the clock signal must be set to high. If the clock is made low the output signal rest as it is irrespective of input signal weather it is low or high. The basic diagram of T flip-flop is shown in figure 6.

TABLE I
T FLIP FLOP TRUTH TABLE

CLK	T	Present state Q_n	Next state Q_{n+1}
1	0	0	0
1	0	1	1
1	1	0	1
1	1	1	0

III. DESIGN OF OPTICAL T FLIP-FLOP

The proposed optical T flip- flop designed is designed in 2D PhCs as shown in figure 7. The T shaped wave guide consists of 16 $\times$ 9 arrays of dielectric rods having refractive index of n=3.44 and of radius 0.19a in the air host of refractive index n=1. The rectangular lattice with a lattice constant a= 0.60μm and controlled junction rods of refractive index n= 3.42 and the rod of radius is 0.32a is used to transmit the maximum power to the output ports with minimum back reflections. The proposed designed consists of three inputs Reference, Clock and T input ports, two output ports Q_n and Q_{n+1}.

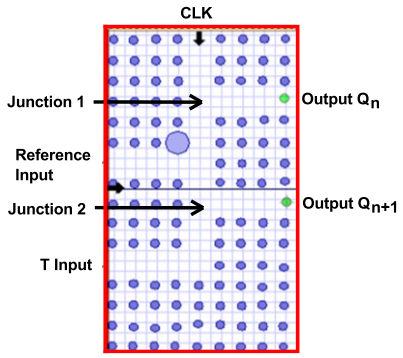

Fig. 7. 2D PhCs lattice structure of optical T flip flop

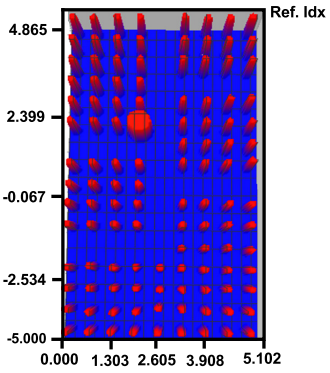

Fig. 8. Refractive index profile of T flip flop

The refractive index profile and PBG is obtained from the stucture as shown in the figure 8 and 9 respectively. The refractive index profile provides the information of light wave travelling inside the 2D structure with an approriate refractive index variation method. The PBG is computed using PWE method as discussed in section II B helps in deciding what operating wavelength the proposed structure is working and also we can vary the PBG so that it will operate in free space wavelength of 1550 nm which has reported very less attenuation for all communication applications.

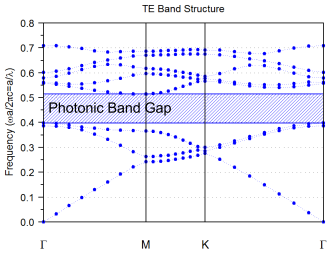

Fig. 9. PBG of T flip flop

IV. RESULTS AND DISCUSSION

The proposed T flop flop designed in 2D PhCs and all the computations are analysed using FDTD and PWE method. As we discussed the in the design section the T flip flop has one input and two outputs to obtain the the output when no input power is applied so we need a reference input to provide optical power to the output waveguide. The Fullwave FDTD analysis is carried out to check all the case logic inputs and verified the outputs in terms of optical power measured at the output waveguide in the optical monitor. The following resutls are are obtained using Opti-FDTD simulation methods.

Case 1: Ref=1, CLK=1, T=0, Q_n=0, Q_{n+1}=0

The input port T exhibits inactive signal and the reference (with a phase of 180°) and CLK signal is made high as shown in figure 10 (a). As a result the output ports Q_n and Q_{n+1} experiences a weak signal as shown in figure 10 (b) and (c) as input T signal is low with a phase of zero.

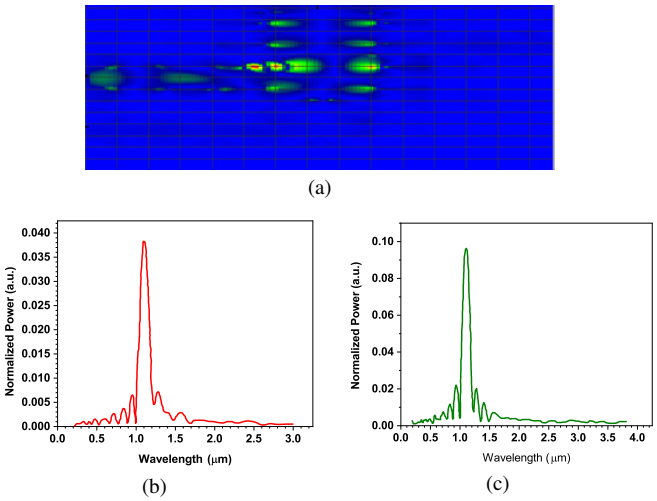

Fig. 10. Simulation result for Ref=1, CLK=1,T=0 and Q_n=0:
(a) electrical field distribution, (b) output at Q_n =0.038, (c) OUTPUT at Q_{n+1}=0.09

Case 2: Ref=1, CLK=1, T=0, Q_n=1, Q_{n+1}=1

The input ports that is reference, and CLK signal is made high and T input signal is set as low as shown in figure 11 (a) .So the junction 1 and junction 2 experiences constructive interference of reference and CLK signal. So we can observe the high output at output ports Q_n and Q_{n+1} as shown in figure 11 (b) and (c).

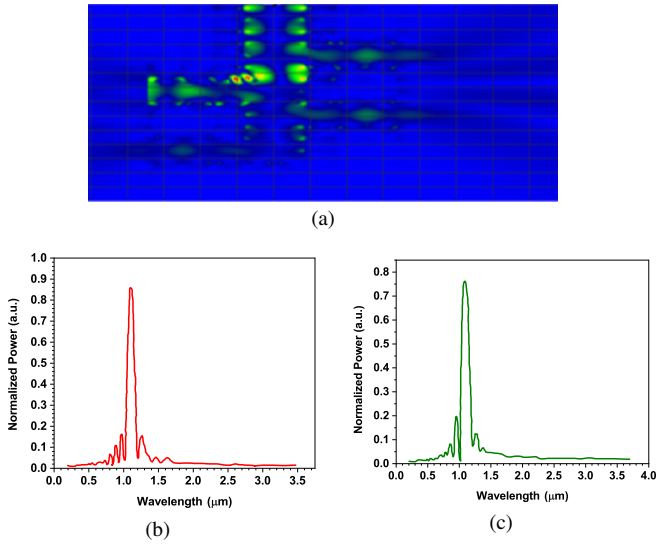

Fig. 11. Simulation result for Ref=1, CLK=1,T=0 and Q_n=0:
(a) electrical field distribution, (b) output at Q_n =0.86, (c) OUTPUT at Q_{n+1}=0.77

Case 3: Ref=1, CLK=1, T=1, Q_n=0, Q_{n+1}=1

T input signal is made high along with reference input signal and CLK signal as shown in figure 12 (a). According to the interference phenomenon, the CLK input signal and the reference signal interfere destructively at first junction 1. As a result we can observe low outputs at Q_n and the signals CLK and T input interfere constructively at junction 2 as a result we get high output at Q_{n+1} as shown in figure 12(b) and (c).

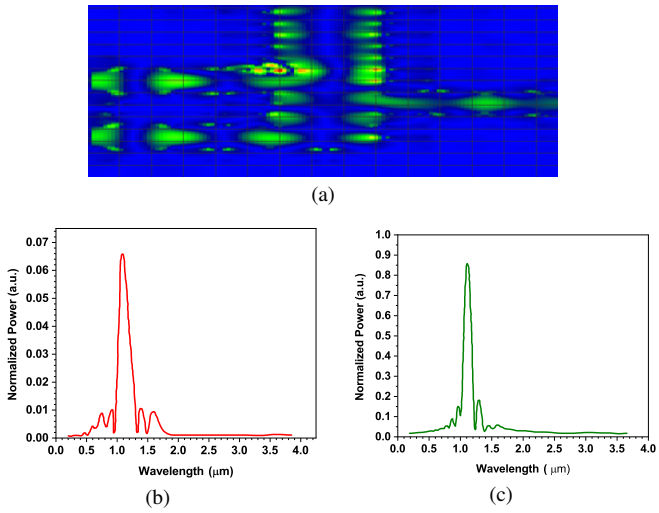

Fig. 12. Simulation result for Ref=1, CLK=1,T=1 and Q_n=0
(a) Electrical field distribution, (b) output at Q_n =0.06, (c) OUTPUT at Q_{n+1}=0.86

Case 4: Ref=1, CLK=1, T=1, Q_n=1, Q_{n+1}=0

In case 4, reference, clock and T input signals are made high as shown in figure 13 (a). According to the interference phenomenon constructive interference takes place at junctions 1 and junction 2 experience destructive interference so we can observe the high output at Q_n output port and low output at Q_{n+1} output port as shown in figure 13 (b) and (c).

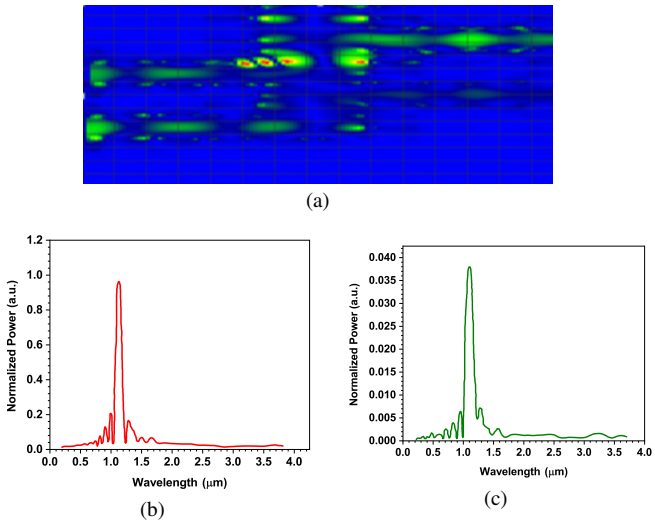

Fig. 13. Simulation result for Ref=1, CLK=1,T=1 and Q_n=1
(a) Electrical field distribution, (b) output at Q_n =0.96, (c) OUTPUT at Q_{n+1}=0.038

The response time is denoted by T_r which is the total time seized by the output to reach 90% of its peak value and is given by T_r = t_d+t_r+t_f where t_d is the delay time and is measured as time taken by the output from 0 to 10% of its maximum value, t_r is the rise time and is measured as time taken by the output to rise from 10% to 90% of its peak value and t_f is the fall time which is normally equal to t_r so T_r = t_d+2t_r . Distance in μs to rise the output from 0 to 10% of its max value is 1.4μs so t_d is equal to 0.0046ps and distance in μs to rise the output from 10% to 90% of its max value is 0.045μs so t_r is equal to 0.00015ps. The T_r= 0.0046ps+ 2*0.00015ps which is equal to o.0049ps. The designed optical T Flip-flop has been evaluated for various values of rod radius and calculated the contrast ratio. The maximum contrast ratio we obtained at the rod radius of 0.114. As shown in the figure 14.

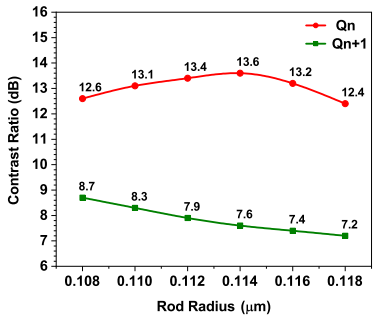

Fig. 14. Contrast ratio of designed T Flip-flop For distant values of Rod radius

TABLE II
OBTAINED T FLIP FLOP VALUES

CLK	T	Present state Q_n	Next state Q_{n+1}
1	0	0.038	0.09
1	0	0.86	0.77
1	1	0.06	0.86
1	1	0.96	0.038

TABLE III
COMPARISION TABLE

References	Lattice Structure	Contrast Ratio (dB)	Area (μm^2)	Response Time (ps)
[28]	Square	14.78	55.08	–
[29]	Square	5.02	–	–
Proposed work	Rectangular	13.60	49.5	0.0049

V. CONCLUSION

The proposed optical T flip flop has designed in 2D PhCs utilizes very less chip area of 49.5μm^2 and the contrast ratio gained is 13.60 dB with very less response and delay time .The proposed design is extremely straightforward and minimal loss of power. These characteristics make it appropriate to apply this optical T flip-flop in photonic coordinated circuits and optical handling at networks.

REFERENCES

[1] S. Swarnakar, S. Rathi, and S. Kumar, "Design of all optical xor gate based on photonic crystal ring resonator," *Journal of Optical Communications*, vol. 41, no. 1, pp. 51–56, 2019. [Online]. Available: https://doi.org/10.1515/joc-2017-0142

[2] A. Pashamehr, M. Zavvari, and H. Alipour-Banaei, "All-optical and/or/not logic gates based on photonic crystal ring resonators," *Frontiers of Optoelectronics*, vol. 9, pp. 578–584, 2016. [Online]. Available: https://doi.org/10.1007/s12200-016-0513-7

[3] J. Bao, J. Xiao, L. Fan, X. Li, Y. Hai, T. Zhang, and C. Yang, "All-optical nor and nand gates based on photonic crystal ring resonator," *Optics communications*, vol. 329, pp. 109–112, 2014. [Online]. Available: https://doi.org/10.1016/j.optcom.2014.04.076

[4] S. Kumar, L. Singh, and N.-K. Chen, "Design of all-optical universal gates using plasmonics mach-zehnder interferometer for wdm applications," *Plasmonics*, vol. 13, pp. 1277–1286, 2018. [Online]. Available: https://doi.org/10.1007/s11468-017-0631-0

[5] K. Choudhary and S. Kumar, "Design of an optical or gate using mach-zehnder interferometers," *Journal of Optical Communications*, vol. 39, no. 2, pp. 161–165, 2018. [Online]. Available: https://doi.org/10.1515/joc-2016-0131

[6] D. G. Sankar Rao, S. Swarnakar, and S. Kumar, "Performance analysis of all-optical nand, nor, and xnor logic gates using photonic crystal waveguide for optical computing applications," *Optical Engineering*, vol. 59, no. 5, pp. 057 101–057 101, 2020. [Online]. Available: https://doi.org/10.1117/1.OE.59.5.057101

[7] B. R. Singh and S. Rawal, "Photonic-crystal-based all-optical not logic gate," *JOSA A*, vol. 32, no. 12, pp. 2260–2263, 2015. [Online]. Available: https://doi.org/10.1364/JOSAA.32.002260

[8] M. V. Sonth, G. Srikanth, P. Agrawal, and B. Premalatha, "Basic logic gates in two dimensional photonic crystals for all optical device design," *International Journal of Electronics and Telecommunications*, vol. 67, no. 2, pp. 247–261, 2021. [Online]. Available: https://doi.org/10.24425/ijet.2021.135972

[9] N. Nozhat and N. Granpayeh, "All-optical logic gates based on nonlinear plasmonic ring resonators," *Applied optics*, vol. 54, no. 26, pp. 7944–7948, 2015. [Online]. Available: https://doi.org/10.1364/AO.54.007944

[10] M. V. Sonth, S. Gowre, N. Biradar, and B. Gadgay, "Design and simulation of and-or-invert logic for photonic integrated circuits," in *Information, Photonics and Communication: Proceedings of Second National Conference, IPC 2019*. Springer, 2020, pp. 55–63. [Online]. Available: https://doi.org/10.1007/978-981-32-9453-0_6

[11] S. Soma, M. V. Sonth, and S. C. Gowre, "Tunable optical add/drop filter for cwdm systems using photonic crystal ring resonator," *Journal of Electronic Materials*, vol. 48, pp. 7460–7464, 2019. [Online]. Available: https://doi.org/10.1007/s11664-019-07572-1

[12] T. Daghooghi, M. Soroosh, and K. Ansari-Asl, "Slow light in ultra-compact photonic crystal decoder," *Applied Optics*, vol. 58, no. 8, pp. 2050–2057, 2019.

[13] M. Maleki, M. Soroosh, and A. Mir, "Ultra-fast all-optical 2-to-4 decoder based on a photonic crystal structure," *Applied Optics*, vol. 59, no. 18, pp. 5422–5428, 2020. [Online]. Available: https://doi.org/10.1364/AO.392933

[14] M. A. Mansouri-Birjandi and M. R. Rakhshani, "A new design of tunable four-port wavelength demultiplexer by photonic crystal ring resonators," *Optik*, vol. 124, no. 23, pp. 5923–5926, 2013. [Online]. Available: https://doi.org/10.1016/j.ijleo.2013.04.128

[15] S. Serajmohammadi, H. Alipour-Banaei, and F. Mehdizadeh, "Application of photonic crystal ring resonators for realizing all optical demultiplexers," *Frequenz*, vol. 72, no. 9-10, pp. 465–470, 2018. [Online]. Available: https://doi.org/10.1515/freq-2017-0272

[16] R. Talebzadeh, M. Soroosh, Y. S. Kavian, and F. Mehdizadeh, "Eight-channel all-optical demultiplexer based on photonic crystal resonant cavities," *Optik*, vol. 140, pp. 331–337, 2017. [Online]. Available: https://doi.org/10.1016/j.ijleo.2017.04.075

[17] M. V. Sonth, S. Soma, S. C. Gowre, and N. Biradar, "Modeling and optimization of optical half adder in two dimensional photonic crystals," *Journal of Electronic Materials*, vol. 47, no. 7, pp. 4136–4139, 2018.

[18] M. V. Sonth, S. Soma, and S. C. Gowre, "Investigation of light behavior of all optical full adders in two-dimensional photonic crystals," *Microwave and Optical Technology Letters*, vol. 63, no. 4, pp. 1304–1308, 2021. [Online]. Available: https://doi.org/10.1002/mop.32705

[19] T. Abdel Moniem, E. Seraj El Deen, and R. El Mayet, "Design of integrated all optical jk flip flop using 2d photonic crystals," *JES. Journal of Engineering Sciences*, vol. 52, no. 4, pp. 62–72, 2024. [Online]. Available: https://doi.org/10.21608/jesaun.2024.278058.1320

[20] Y. Pugachov, M. Gulitski, and D. Malka, "Photonic crystal flip-flops: recent developments in all optical memory components," *Materials*, vol. 16, no. 19, p. 6467, 2023.

[21] T. A. Moniem, E. S. El Deen, and R. El Mayet, "Design of integrated all optical jk flip flop using 2-d photonic crystals." *Journal of Engineering Sciences*, vol. 52, no. 4, 2024. [Online]. Available: https://doi.org/10.21608/jesaun.2024.278058.1320

[22] Y. Pugachov, M. Gulitski, and D. Malka, "Design of all-optical d flip flop memory unit based on photonic crystal," *Nanomaterials*, vol. 14, no. 16, p. 1321, 2024.

[23] S. Soma, M. V. Sonth, and S. C. Gowre, "Design of two-dimensional photonic crystal based ultra compact optical rs flip-flop," *Photonic Network Communications*, vol. 43, no. 2, pp. 109–115, 2022. [Online]. Available: https://doi.org/10.1007/s11107-021-00955-7

[24] S. Kumar, G. Singh, A. Bisht, and A. Amphawan, "Design of d flip-flop and t flip-flop using mach–zehnder interferometers for high-speed communication," *Applied optics*, vol. 54, no. 21, pp. 6397–6405, 2015.

[25] K. Huybrechts, G. Morthier, and R. Baets, "Fast all-optical flip-flop based on a single distributed feedback laser diode," *Optics Express*, vol. 16, no. 15, pp. 11 405–11 410, 2008.

[26] K. M. Rao, P. S. Bharadwaj, S. M. Vali, N. Mahesh, and T. T. Sai, "Design of clocked hybrid (d/t) flip-flop through air hole paradigm photonic crystal," *Journal of VLSI circuits and systems*, vol. 3, no. 2, pp. 21–33, 2021.

[27] H. Miyan, R. Agrahari, S. K. Gowre, P. K. Jain, and M. Mahto, "Computational study of 2d photonic crystal based biosensor for sars-cov-2 detection," *Measurement Science and Technology*, vol. 34, no. 7, p. 074004, 2023. [Online]. Available: https://doi.org/10.1088/1361-6501/acc754

[28] D. G. S. Rao, V. Palacharla, S. Swarnakar, and S. Kumar, "Design of all-optical d flip-flop using photonic crystal waveguides for optical computing and networking," *Applied Optics*, vol. 59, no. 23, pp. 7139–7143, 2020. [Online]. Available: https://doi.org/10.1364/AO.400223

[29] M. Valliammai, J. Mohanraj, T. Kanimozhi, and S. Sridevi, "Design of all-optical chalcogenide t-flip flop using photonic crystal waveguide," in *2021 International Conference on Numerical Simulation of Optoelectronic Devices (NUSOD)*. IEEE, 2021, pp. 133–134. [Online]. Available: https://doi.org/10.1109/NUSOD52207.2021.9541504